

## Title

# **PGC1 $\alpha$ agonist rescues doxorubicin induced cardiomyopathy by mitigating the oxidative stress and necroptosis**

## Introduction

Majority of the cardiomyopathy cases advances into heart failure, where terminal treatment is heart transplantation, which is challenging due to limited availability of donors. Among cardiomyopathy the largest prevalence is of DCM phenotype, which accounts for more than 50% of heart transplantation cases [1] and is characterized by increased ventricular dimensions, thinning of chamber walls, reduction in ejection fraction and overall compromised systolic function. DCM can be genetic, acquired, drug induced or idiopathic [2].

Owing to significant cardiotoxicity properties, use of chemotherapeutic drug like DOX is a major concern among cancer patients. The DOX treated patients often presented with many life threatening cardiovascular complications, prominent among which is cardiomyopathy (or DCM) [3]. Clinically, the DOX induced cardiomyopathy is having similar morphological and functional derangements in the cardiac tissue to those of DCM that eventually culminating to HF. However, despite extensive research, the precise mechanism of DOX induced cardiomyopathy (or DCM) is not yet completely understood. Cell death is the most unifying event that occurs in majority of heart injuries associated with disease conditions like ischemia-reperfusion, cardiomyopathy, myocardial infarction, heart failure including DOX. The three well known causative factors of cell death are, (i) excessive oxidative stress due to massive production of reactive oxygen species (ROS); (ii) interaction of DOX with topoisomerase-  $\alpha$  and  $\beta$  by DNA intercalation thereby causing double strand breaks and hindering transcription machinery; (iii) mitochondrial damage [4-8].

Besides apoptosis, there are various cell death mechanisms that have been explained as regulated cell death pathways e.g. autophagy, necroptosis, pyroptosis and ferroptosis [9, 10]. In recent studies, above mentioned cell death pathways have been widely associated with DOX induced cardiomyopathy [11] but which cell death pathway predominantly triggered by DOX and the underlying mechanism is not clearly defined. Recently, necroptosis has gained wide attention and its role has been implicated in DOX induced cardiomyopathy/cardiotoxicity [11-13]. Necroptosis has been identified as cell death mechanism that occurred in a programmed way, and it is regulated by kinases i.e. receptor interacting protein kinases (RIPK)-1, RIPK-3, and (mixed-lineage kinase and domain-like pseudokinase (MLKL).

Further, necroptotic cells releases 'alarmin' molecules which act as danger signals for nearby cells [14, 15]. Some of these molecules are ubiquitously present and have important role in cellular functions, but ones outside cells, these act as danger signal for neighboring cells [14]. Alarmins are potent source of inflammation and augments the recruitment of inflammatory immune cells and can also trigger cell death. Enhanced inflammatory milieu at the site of pathology augments oxidative stress leading to exacerbated tissue damage.

Therefore, strategies to annihilate the DOX induced cardiomyopathy via regulating the necroptosis process, alarmin release and reducing oxidative stress are highly warranted and the outcome of such studies may be applied in the management of different types of cardiomyopathies/cardiac injuries to prevent its progression towards HF. Targeting necroptosis resulted in protective effects on doxorubicin-induced cardiotoxicity models [9, 10]. Considering the above facts, in this study we targeted a nuclear encoded transcriptional coactivator i.e. PGC-1 $\alpha$  (peroxisome proliferator-activated receptor gamma ((PPAR- $\gamma$ ) coactivator-1alpha) which is considered as the 'master regulator' of mitochondrial biogenesis and its function. Further, PGC-1 $\alpha$  exerts a strong antioxidant effect [16], regulates cellular energy metabolism, cell growth [17] and its role has also been suggested in driving inflammation and immune regulation [18]. Activation of PGC1 $\alpha$ /SIRT (Sirtuin)1 pathway has been reported to be associated with elevation of autophagy/mitophagy leading to suppression of oxidative stress-mediated ROS production [19]. However, the role of PGC-1 $\alpha$  in regulating necroptosis, alarmin production and oxidative stress in doxorubicin induced cardiomyopathy model has not been described. Therefore, present study employed PGC-1 $\alpha$  agonist (i.e. ZLN005) with an aim to rescue the DOX induced deleterious effects on heart via alleviating the necroptosis and oxidative stress thereby restoring the cardiac function by preventing extensive cardiac tissue remodelling.

## Objectives

- 1) To establish doxorubicin induced model of cardiomyopathy and study baseline levels of molecules associated with alarmins, oxidative stress, necroptosis in control and doxorubicin treated mouse
- 2) To evaluate the role of PGC1 $\alpha$  agonist (ZLN005) in rescuing doxorubicin induced cardiomyopathy model and to evaluate their role in association with alarmins, oxidative stress, necroptosis and cardiac remodeling

## Materials and Methods

### 2.1. Mice and Experimental Procedures

All animal experiments were approved by Institute Animal Ethics Committee, All India Institute of Medical Sciences (AIIMS), New Delhi. C57BL/6 male mouse of 24-27g (8 weeks old) were purchased from Central Animal Facility, AIIMS, Delhi. Mouse were fed ad libitum and were housed under standard 12 h light-dark cycles with controlled temperature and humidity in ventilated rooms. Daily performance of mice, their weight and behavior were recorded. At the end of treatment regime mice were euthanized humanely with overdose of isoflurane. The hearts were perfused, isolated and used for subsequent experiments. Forty mice were randomly divided into four groups i.e. control, DOX, ZLN005 and ZLN005+DOX (n = 10, each group). The doxorubicin model was established as previously described [20]. Briefly, doxorubicin (single dose, 10mg/kg, i.p., Cayman Chemicals, USA) was administered (**Figure 1a**) in DOX group and survival schedule of 7 days was followed. Control mice were administered with vehicle (1X PBS, i.p.). The ZLN005 + DOX group received DOX and ZLN005 whereas ZLN005 group received ZLN005 only. Repeated dosing model was adapted for ZLN005 based intervention [21]. The ZLN005 (four doses of 2.5mg/kg/dose, cumulative dose, 10mg/kg, Cayman Chemicals, USA) was administered i.v., 2hrs after doxorubicin [22] through retro-orbital route every alternate day as demonstrated in **Figure 3a**.

### 2.2. Gene expression by quantitative PCR

Heart tissues were homogenized using mortar and pestle in liquid nitrogen and transferred to TriExtract (G-Biosciences). Total RNA was isolated and quantified followed by DNase treatment (DNase I, RNase-free, ThermoFisher Scientific, CA, U.S.A.). Complementary DNA (cDNA) was synthesized using cDNA synthesis kit (iScript cDNA synthesis kit, BioRad, Hercules, CA, USA) following manufacturer's instructions. The PCR was performed using iTaq Universal SYBR Green Supermix (Biorad, Hercules, CA, USA) in CFX96 Real-time PCR system, (BioRad, Hercules, CA, USA) in accordance to MIQE guidelines. PCR cycles were set for 10 min denaturation, followed by 40 cycles of denaturation at 95°C for 15secs, followed by primer annealing and extension at optimized temperature. Samples were run in triplicates and GAPDH (Glyceraldehyde 3-phosphate dehydrogenase) was used as housekeeping gene for normalization of data. The gene expression data was represented as  $2^{-\Delta C_t}$  for all the groups.

**Table 1.** List of genes and the primers.

S.No.	Gene name	Accession ID	Forward Primer (5'→3') Reverse Primer (5'→3')
1.	<i>CATHEPSIN-B</i>	NM_007798.3	GGCTCTTGTTGGGCATTG CAGCTTCACAGCTCTTGTTGC
2.	<i>HMGB1</i>	NM_001313894.1	TCCCTCATCCTTGTTTACTCG GCAGTTTCCTATCGCTTTGG
3.	<i>RIPK1</i>	NM_001359997.1	AGGTGTCCTTGTTTACC CCTCCACGATTATCCTTCC
4.	<i>RIPK3</i>	NM_019955.2	AAGACAGTCCTTGCCACTTCC TGGGTCAAGAGTCAGTTTGGG
5.	<i>MLKL</i>	NM_001310613.1	ATGCCAGCGTCTAGGAAACC TCGGGCAGGTTCTTCTTTCC
6.	<i>S100B</i>	NM_009115.3	ACAACGAGCTCTCTCACTTCC CATCTTCGTCCAGCGTCTCC
7.	<i>PGC-1<math>\alpha</math></i>	NM_008904.3	GCACACACCGCAATTCTCC AGGCTTCATAGCTGTCGTACC
8.	<i>GAPDH</i>	NM_001411843.1	AACTTTGGCATTGTGGAAGGG CATCACGCCACAGCTTTCC

### 2.3. Immunofluorescence

Freshly isolated mouse hearts were dissected on ice and immediately fixed in 4% paraformaldehyde. Tissue was paraffin embedded and sectioned at 3-5 microns. The sections were deparaffinized followed by antigen retrieval and blocking. Primary antibody incubation with RIPK1 (H-207) (1:500, Santa Cruz), RIPK3 (H-43) (1:500, Santa Cruz), MLKL (1:500, Thermo Fisher Scientific),  $\alpha$ -SMA (1: 500, Abcam), PGC-1 $\alpha$  (1:200, ABclonal) at 4°C was done overnight, followed by washing and secondary antibody incubation with FITC-conjugated goat anti-rabbit (1:500, Abcam) for one hour at room temperature, followed by nuclei counterstain with 4',6-diamidino-2-phenylindole (DAPI) (Sigma Aldrich). Tissue sections were washed and mounted using Vectashield antifade mounting medium (Vector Laboratories, Newark, USA). Images were captured using Nikon Eclipse Ni upright fluorescent microscope (Nikon, Japan) using NIS-Elements Br software (Nikon, Japan). Mean fluorescence intensity of signal and background was calculated using Fiji software (NIH, USA). The data from 4 different sections was used to capture five different fields of views each, which were used for further statistical analysis.

### 2.4. Histological analysis

For Trichome staining sections were deparaffined in decreasing gradient of ethanol, fixed in Bouin's solution (Sisco Research Laboratories Pvt. Ltd., India) overnight. Sections washed in running tap water followed by staining of nucleus using modified Weigert's Iron hematoxylin stain (Sisco Research Laboratories Pvt. Ltd., India) which was washed and staining was proceeded for trichome stain to discriminate between muscle and fibrosis, followed by dehydration and mounting. Similarly, for Picrosirius Red staining the deparaffinized tissue sections were stained using modified Weigert's hematoxylin (Sisco Research Laboratories Pvt. Ltd., India) which was washed to stain for Sirius Red (Sisco Research Laboratories Pvt. Ltd., India) for one hour, which was proceeded by dehydration and mounting of tissue using DPX Mountant (Sigma, USA).

### 2.5. Protein quantification by Enzyme Linked Immune Sorbent Assay (ELISA)

Protein quantification was performed using ELISA. Mouse 8-hydroxy-desoxyguanosine (8-OHdG) (MyBioSource, USA), Malondialdehyde (Elabscience), Catalase (MyBioSource, USA), Superoxide Dismutase (MyBioSource, USA), Glutathione (GSH, yBioSource), Glutathione Reductase (GSSG, (MyBioSource, USA), Collagen-I (MyBioSource, USA), Collagen III (MyBioSource, USA), Fibronectin (MyBioSource, USA), Laminin (MyBioSource, USA) kits were used and all the immunoassay steps were performed as per manufactures instructions. Optical density was measured using Epoch microplate reader (BioTek, Agilent) at 450nm. The concentrations were expressed as picogram (pg) or nanogram (ng) per milliliter (mL).

## Results

Doxorubicin is a widely used chemotherapeutic drug. It demonstrates dose dependent toxicity. We have used an acute cardiotoxicity model with short term survival (**Figure 1a**). Overall the heart showed enhanced dilatation of chambers and higher filling capacity as quantified by histology images (**Figure 1b**). Alterations in cardiac tissue morphology showed enhanced vacuolations, distorted myofibril structure and increased leukocyte infiltration (**Figure 1c**).

We analyzed fibrosis in cardiac tissue by Masson Trichome, Sirius Red and  $\alpha$ -SMA (alpha-smooth muscle actin) staining and significantly increased staining revealed enhanced fibrosis by all the three methods in DOX group compared to controls (**Figure 2a**). Further, necroptosis cell death pathway was analyzed by immunofluorescence based protein localization (and quantification) for key molecules like RIPK1, RIPK3 and MLKL in cardiac tissue. Significantly increased staining ( $p < 0.0001$ ) was observed for all three markers in DOX group compared to controls that was indicative of enhanced necroptosis (Fig 2c and 2d). However, corresponding mRNA levels showed differential expression pattern that were not statistically significant (**Figure 2c**).

We identified PGC1 $\alpha$  agonist i.e. ZLN005 that significantly increased the expression of PGC1 $\alpha$  protein (no significant changes observed at mRNA levels) in the heart tissue (**Figure S1, supplementary data**). In order to rescue the DOX induced cardiomyopathy phenotype, we treated mice with ZLN005 as mentioned in above section (**Figure 3a**). We observed remarkable recovery in myocardial mass, reduced dilatation of heart and vacuolations with overall improvement in structural integrity in ZLN005+DOX group compared to DOX group (**Figure 3b and 3c**). Weight reduction, a critical parameter to determine the overall health and metabolism of mice also revealed significant improvement in ZLN005+DOX group when compared to doxorubicin treated group (**Figure 3d**). Further, marked decrease in Masson's Trichome, Sirius Red and  $\alpha$ -SMA staining (**Figure 4a**) were observed in ZLN005+DOX treated group compared to DOX group. Significant reduction ( $p < 0.0001$ ) in immunofluorescence based protein localization of necroptosis markers was observed in ZLN005+DOX treated group compared to DOX group indicating enhanced survival of cardiomyocytes attributed by PGC-1 $\alpha$  agonist (**Figure 4c and 4d**). However, no significant difference was observed in the corresponding transcript levels when compared all three groups (**Figure 4b**). Next, the transcript expression levels of alarmin molecules i.e.

HMGB1, S100b and Cathepsin-B were determined but statistically significant difference was not observed for all three studied genes in all four groups (**Figure 5**).

Since DOX triggered a potent oxidative stress response, we further investigated the status of hallmark markers associated with oxidative stress response to understand the ZLN005 effect. We analysed the levels of 8-OHdG (a marker of DNA damage) (**Figure 6a and 6b**) and MDA (a lipid peroxidation marker) that were found to be significantly increased in DOX group compared to controls ( $p<0.0001$ ) and corresponding levels were significantly reduced in ZLN005+DOX ( $p=0.0004$  for 8-OHdG and  $p=0.016$  for MDA) but remained higher compared to control group. Conversely, the ROS (reactive oxygen species) scavenging enzyme i.e. SOD and catalase activities were significantly decreased in DOX group compared to control ( $p<0.0001$ ) and activities of same were increased after ZLN005 treatment (DOX+ZLN005 group) but they were comparable to control group (**Figure 6c and 6d**). Similarly, glutathione (GSH) levels and Glutathione Reductase (GSSG) were respectively decreased ( $p=0.003$ ) and increased ( $p=0.004$ ) in DOX group compared to control, while contrasting trends were observed in DOX+ZLN005 group (**Figure 6e and 6f**) compared to DOX group. Likewise, the GSH:GSSG ratio was decreased DOX group compared to control ( $p=0.001$ ) and it was restored to normal in DOX+ZLN005 group ( $p=0.001$ ) (**Figure 6g**).

Based on high  $\alpha$ -SMA and fibrosis staining that indicated significant tissue remodeling, we further investigated the effect on cardiac tissue remodeling by quantifying the levels of key extracellular matrix proteins involved in structural homeostasis i.e. Laminin, fibronectin, collagen I and collagen III. We observed significant upregulation of laminin and fibronectin in DOX group compared to control group ( $p<0.0001$ ) but their levels remained comparable to control in ZLN005+DOX group, (**Figure 6h and 6i**). Next, as expected the collagen-I and collagen III were significantly decreased and increased respectively in DOX group ( $p<0.0001$ ) compared to controls, but these alterations were preserved by ZLN005 treatment as evident by ratio of collagen I to collagen III (**Figure 6l**). In all the above studied parameters, the control groups were found comparable to ZLN005 group.

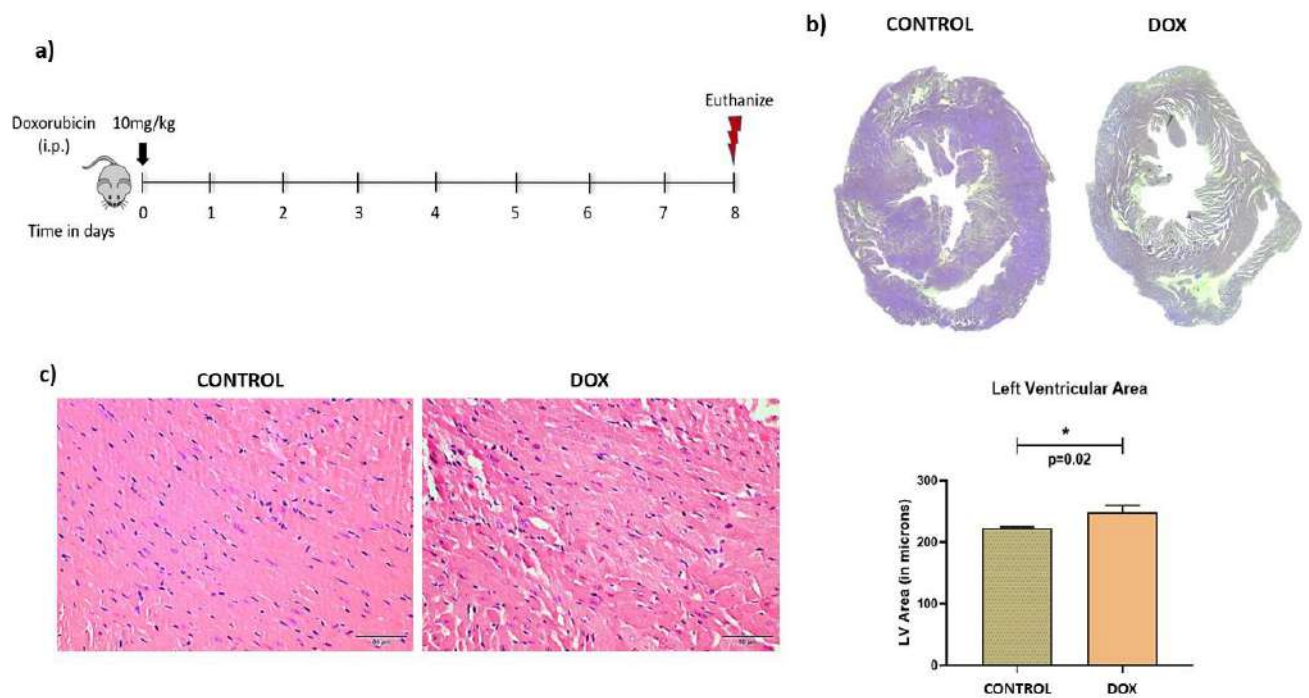


**Figure 1.** Doxorubicin induced model of cardiomyopathy. **a)** Schematic diagram of dose schedule for doxorubicin induced cardiomyopathy model. **b)** Micrograph of cardiac tissue (upper panel) and quantification of Left ventricular Volume (lower panel). **c)** Hematoxylin and eosin staining of control and doxorubicin treated heart. Scale bar = 50  $\mu$ m, (\*) =  $p < 0.05$ .

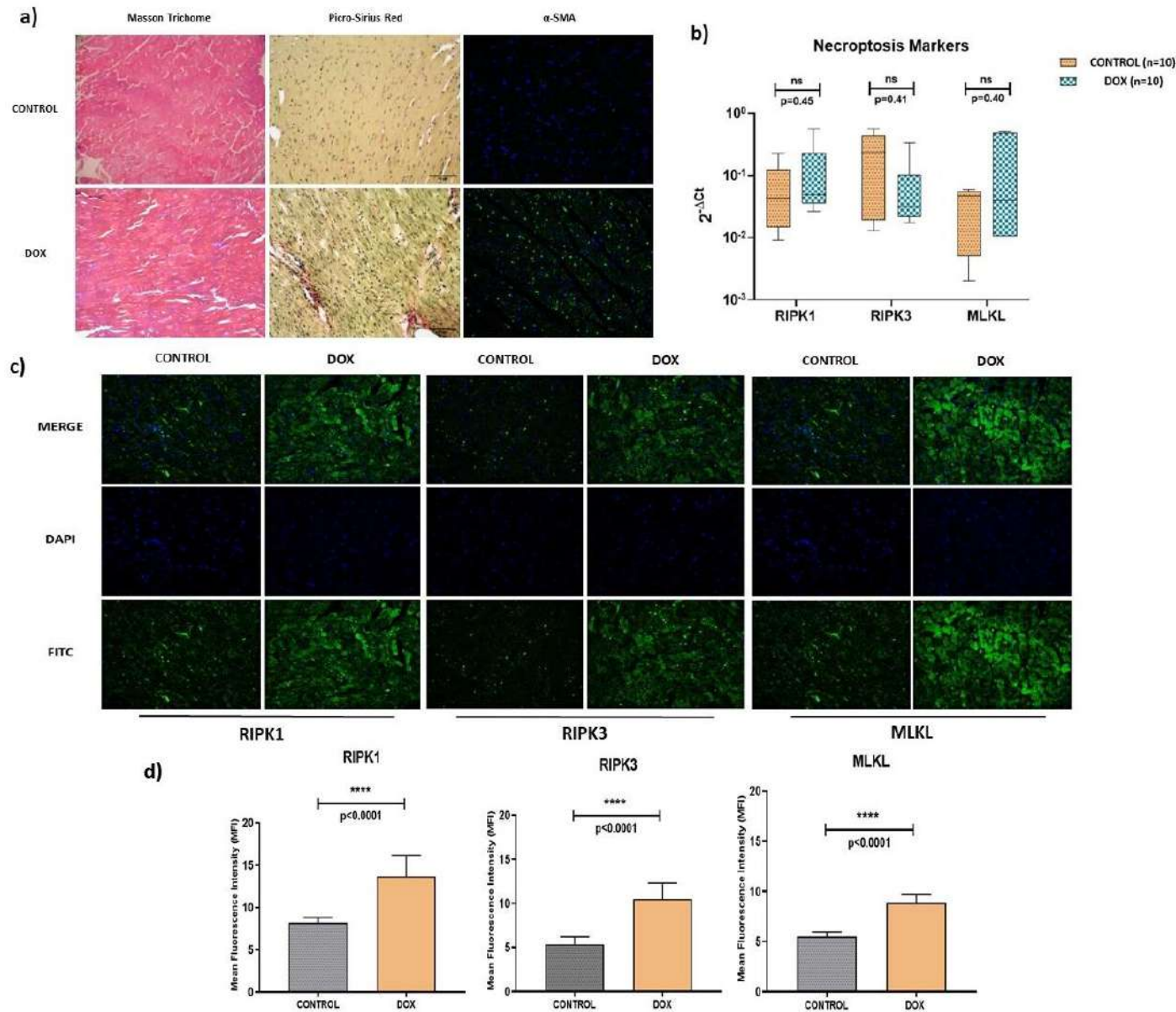


**Figure 2.** **a)** Analysis of cardiac tissue fibrosis via Masson Trichome Staining (Muscle tissue = pink to red, Collagen deposition = Blue and Nucleus = Black), Picro-Sirius Red staining (Muscle tissue and cell cytoplasm = yellow, collagen deposits = Red and nucleus = black) and  $\alpha$ -SMA (blue = nucleus and green =  $\alpha$ -SMA). **b)** qPCR based transcripts expression for necroptosis markers (RIPK1, RIPK3, MLKL). **c)** Immunofluorescence of Necroptosis markers (RIPK1, RIPK3 and MLKL) in control and doxorubicin treated groups. **d)** Quantification of immunofluorescence data. ns= non-significant, (\*) =  $p < 0.05$ , (\*\*) =  $p < 0.01$ , (\*\*\*) =  $p < 0.001$ , (\*\*\*\*) =  $p < 0.0001$ .

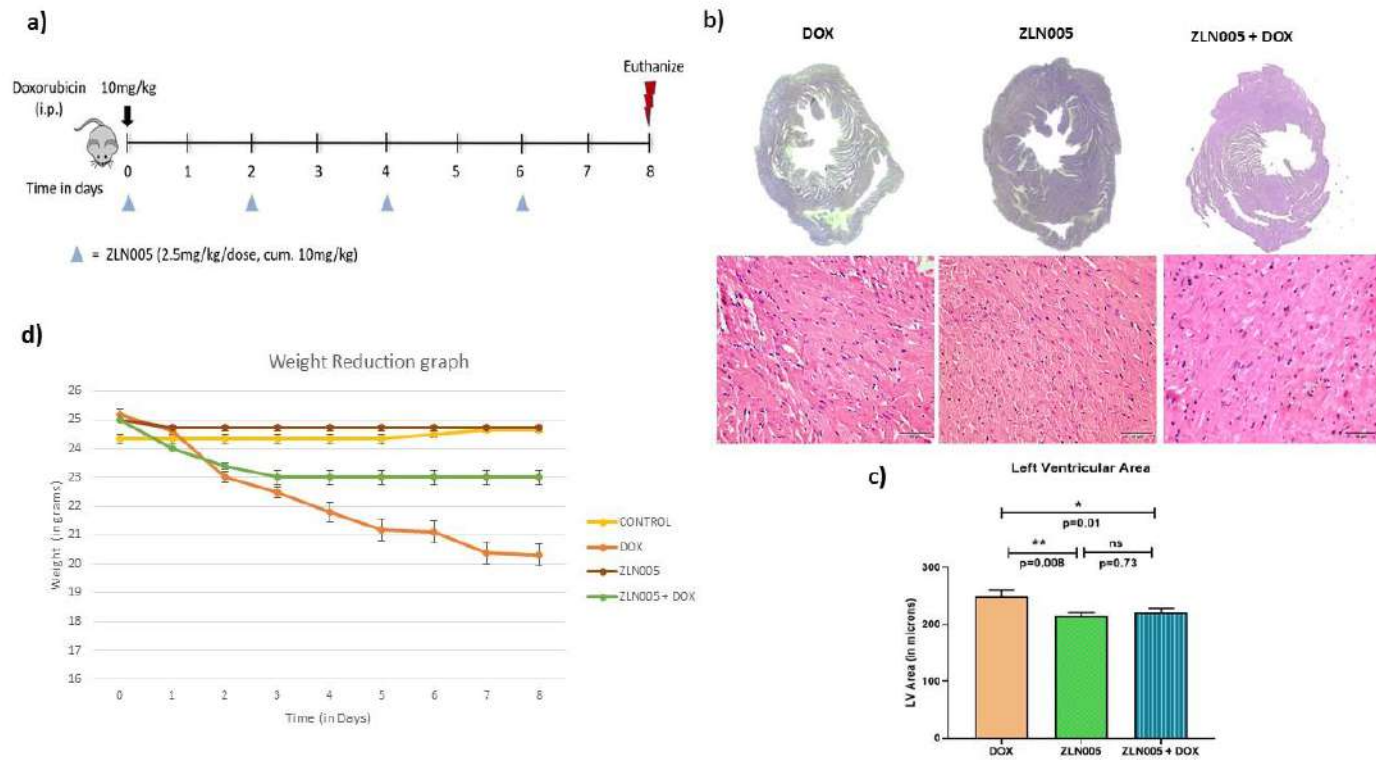


**Figure 3.** PGC-1 $\alpha$  agonist (ZLN005) based intervention to rescue doxorubicin induced model of cardiomyopathy. **a)** Schematic diagram of dose schedule for ZLN005 based intervention in doxorubicin induced cardiomyopathy model. **b)** Micrograph of cardiac tissue (top) and haematoxylin and eosin staining (bottom) of doxorubicin treated heart and intervention group. Scale bar = 50 $\mu$ m. **c)** Quantification of Left ventricular Volume. **d)** Comparison of body weights of mice with time (in days) in all the study groups, (\*) =  $p < 0.05$ .



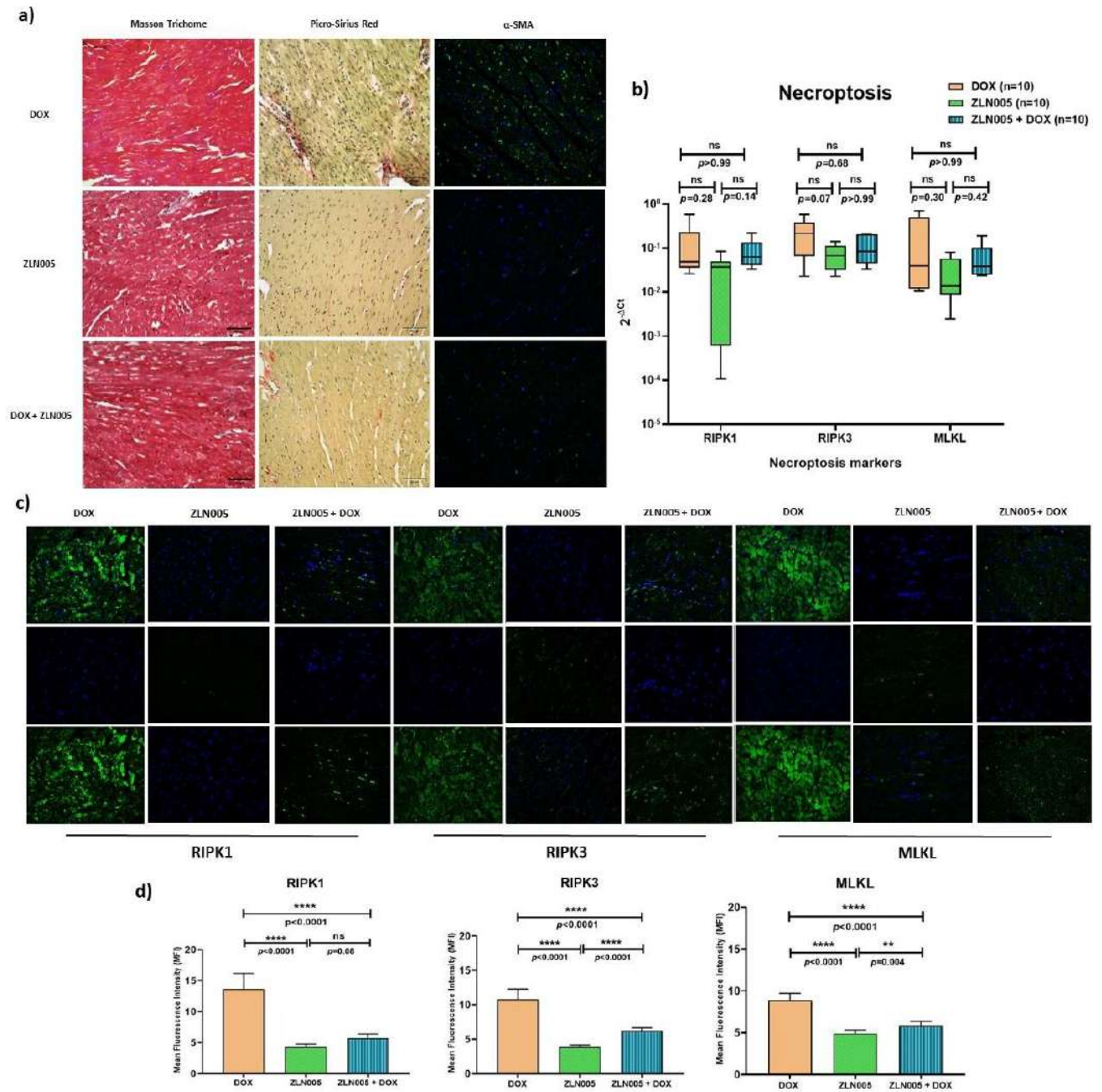


**Figure 4.** **a)** Analysis of fibrosis via Masson Trichome Staining (Muscle = pink to red, Collagen = Blue and Nucleus = black), Picro-Sirius Red staining (Muscle tissue and cell cytoplasm = yellow, collagen = red strands and nucleus = black) and  $\alpha$ -SMA (blue = nucleus and green = staining of  $\alpha$ -SMA) in Dox, ZLN005 and ZLN005+Dox groups. **b)** qPCR based transcripts expression for necroptosis markers (RIPK1, RIPK3, MLKL). **c)** Immunofluorescence of Necroptosis markers (RIPK1, RIPK3 and MLKL) in study groups. **d)** Quantification of immunofluorescence data. ns= non-significant, (\*) =  $p < 0.05$ , (\*\*) =  $p < 0.01$ , (\*\*\*) =  $p < 0.001$ , (\*\*\*\*) =  $p < 0.0001$ .



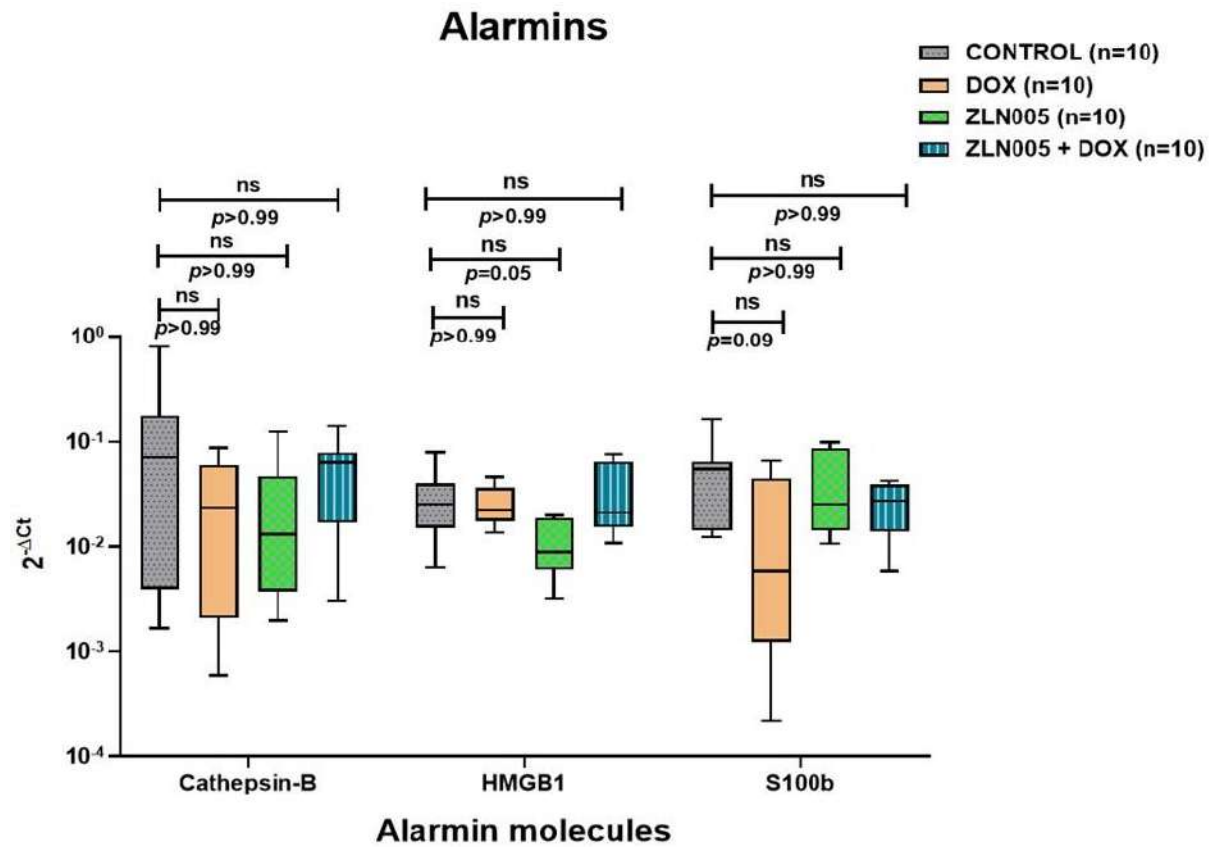


**Figure 5.** Transcript expression levels (qPCR) of alarmin molecules in control, Dox, ZLN005 and ZLN005+Dox hearts. ns= non-significant (significant  $p$  value is set as  $p < 0.05$ ).

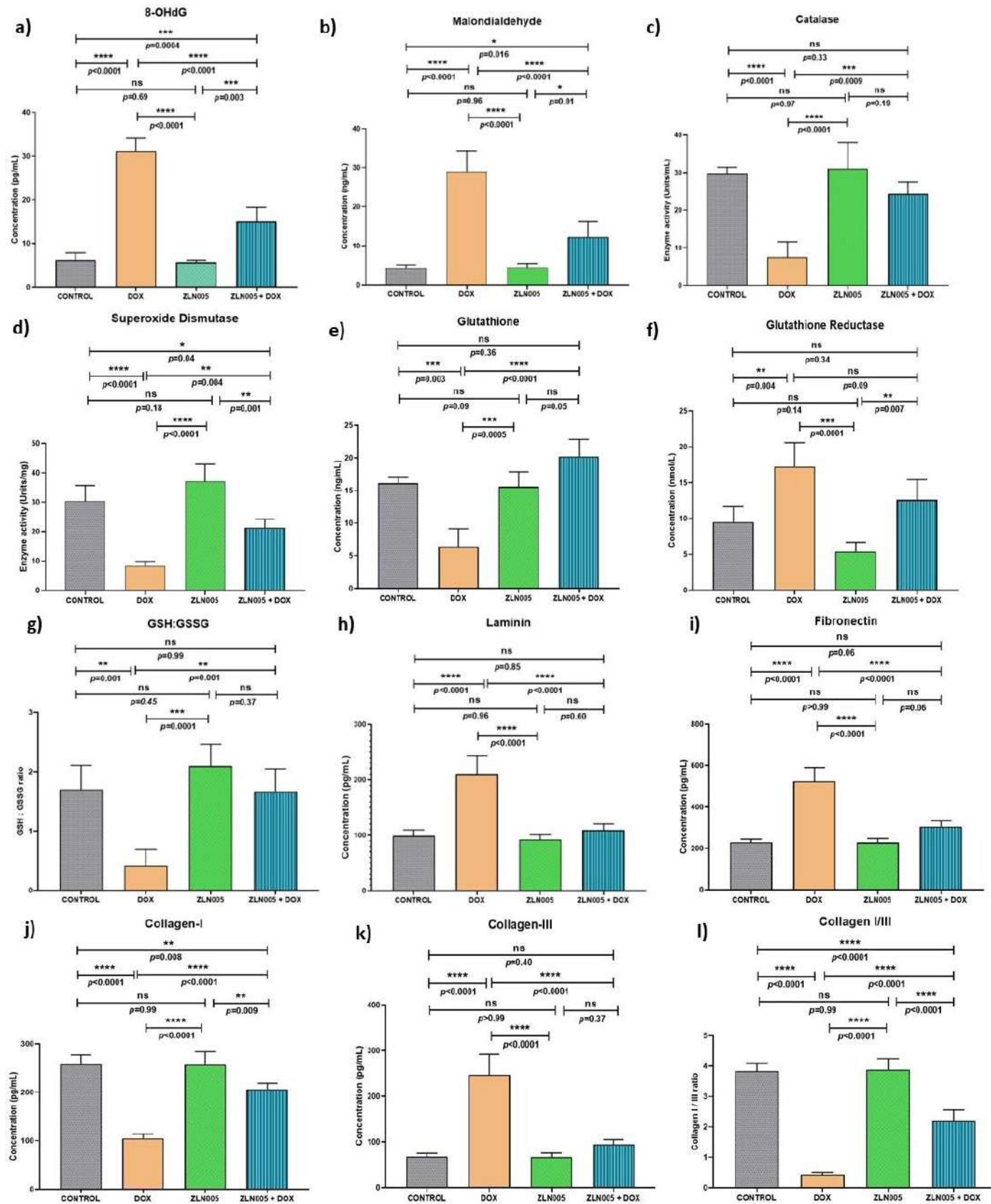


**Figure 6. a-g)** Status of Oxidative stress markers in cell lysates of cardiac tissue of control, Dox, ZLN005 and ZLN005+Dox groups. **h- l)** Tissue remodeling parameters for cardiac cell lysates of all the study groups. 8-OHdG = (8-oxo-7,8,-dihydro-2'-deoxyguanosine). (\*)=  $p < 0.05$ , (\*\*)=  $p < 0.01$ , (\*\*\*)=  $p < 0.001$ , (\*\*\*\*)=  $p < 0.0001$ .

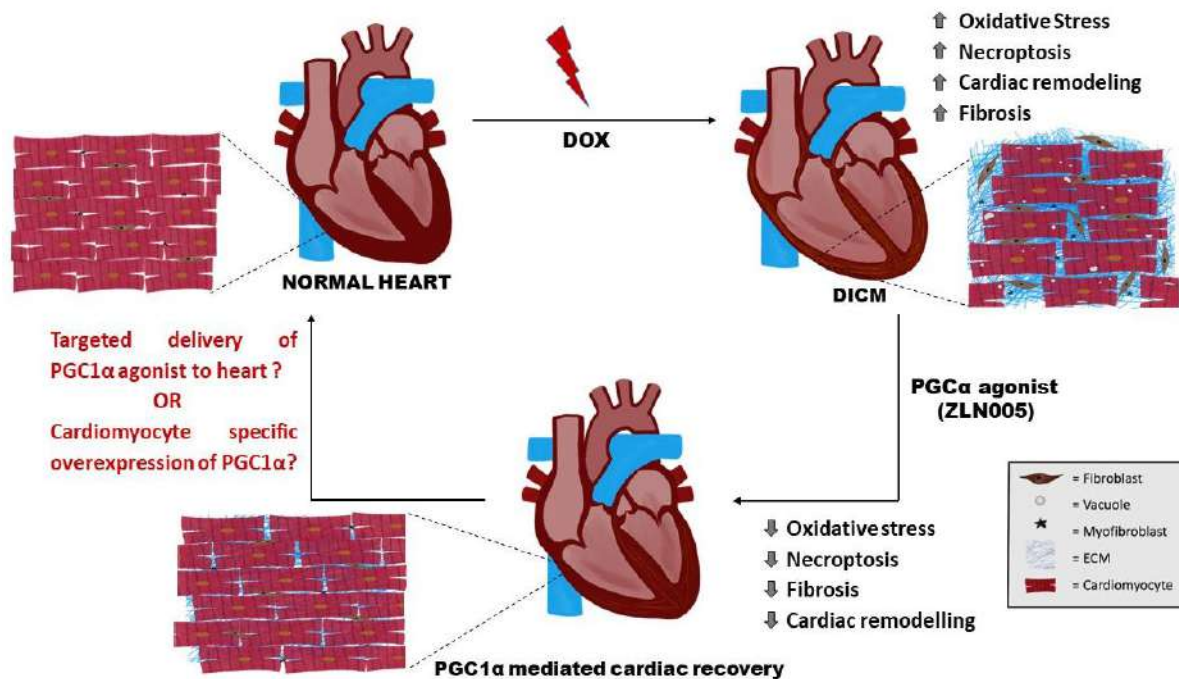


**Figure 7.** Schematic representation of DOX induced cardiotoxic effects (enhanced oxidative stress, necroptosis, fibrosis and cardiac remodeling) which was mitigated by PGC1 $\alpha$  agonist i.e. ZLN005. (? = require further investigation). DOX= doxorubicin, DICM = DOX induced cardiomyopathy.

## Statistical Analysis

All data was analyzed using graph Pad Prism 8 (GraphPad Software, Inc., San Diego, CA, USA). Data was analyzed for normality using D'Agostino and Pearson test, Shapiro-Wilk test, Kolmogorov-Smirnov test and visually validated by plotting Q-Q plot. Mann Whitney U test was done for non-parametric tests (qPCR data). One-way ANOVA (ELISA data) and unpaired t test (Immunofluorescence images quantification) was performed for normally distributed data. Significance test was performed using p-value of <0.05, error bars indicated mean  $\pm$  SD (standard deviation). All experiments were performed in triplicates and the average was used for subsequent analysis.

## Discussion

Heart failure (HF) remains a global health issue that requires development of newer treatment strategies to combat the alarmingly increasing disease burden. As mentioned above significant proportion of cancer survivors who received chemotherapy (e.g. DOX) were also presented with various types of cardiomyopathies [4-6] and at present dexrazoxane is the only clinically approved agents used to minimize the DOX induced cardiotoxicity [12].

Since DOX causes mitochondrial dysfunction and mitochondrial homeostasis is critical to meet the high energy demand of a dynamic organ like heart [23, 24], it is imperative to target a molecule that will compensate the DOX mediated toxic effect on mitochondrial dynamics along with reducing the oxidative stress and cell death.

As described earlier, PGC1 $\alpha$  is a master regulator of mitochondrial biogenesis and it is also essential for the cardiomyocytes during developmental stages. It has been reported as a crucial factor for differentiation/maturation of human embryonic stem cells (hESC) into cardiomyocyte phenotype [25] and it is also known to regulate the respiration process in hiPSC (human induced pluripotent stem cells) generated cardiomyocytes [26]. Role of PGC1 $\alpha$  in mitigating cardiac injury is however, not well defined particularly in context with necroptosis, oxidative stress and cardiac tissue remodeling. Decreased PGC1 $\alpha$  expression is reported in doxorubicin induced model of cardiotoxicity [8] and in *in vitro* models of cardiac hypertrophy [27]. Further, enhancing PGC1 $\alpha$  in renal I/R injury model was able to reverse fibrosis [28] and rescue nephrotoxicity. Similar observations were observed in neurotoxicity I/R model [22]. Liang et al. reported that the oxidative damage and mitochondrial dysfunction induced by H<sub>2</sub>O<sub>2</sub> exposure in IPEC-1 intestinal cells has been ameliorated by activation of PGC1 $\alpha$ /SIRT1 pathway *via* upregulating autophagy/mitophagy [19] indicating the

critical role of PGC1 $\alpha$  in regulating oxidative stress and mitochondrial function. Therefore, we employed a PGC1 $\alpha$  agonist with an aim to rescue the DOX induced cardiomyopathy like phenotype. Our findings revealed an increased cardiac tissue mass and improved structural changes with reduced vacuolations and fibrosis pointing towards overall improvement in DOX induced injury and the data was found in agreement with above mentioned studies in different disease models. Since, PGC1 $\alpha$  possess potent anti-oxidant properties and its role has been demonstrated in regulating the cellular growth and mitochondrial antioxidant defense system in distinct cell types under various stressors influence/disease conditions [16, 19, 29, 30]. In the present study ZLN005 treatment mitigated the harmful effects of DOX induced oxidative stress (kept *status quo* with control group) with corresponding improvement in cardiac fibrosis and preserved structural integrity.

Enhanced activities of free radical scavenging enzymes i.e., Catalase, SOD and GSH and decreased concentration of 8-OHdG (DNA damage marker), MDA (lipid peroxidation marker) and GSSH observed in ZLN005 intervention (ZLN005+DOX) group compared to DOX group and levels of catalase, glutathione, glutathione reductase, GSH:GSSG ratio of ZLN005+DOX group was found comparable to control group.

8-OHdG increases with oxidative stress and ROS accumulation, thereby contributing to DNA damage and is related to cardiovascular disease onset and progression [31, 32]. Status of key antioxidant enzymes including catalase, glutathione and superoxide dismutase were enhanced in ZLN005+DOX group. Catalase overexpression in heart prevents progression into heart failure and influences myocardial remodeling by reducing fibrosis [33]. The SOD serves as first line of defense against ROS and SOD levels related to adverse LV geometry and progression towards HF [34] and similar findings were observed in the DOX model of present study. Increased SOD levels are associated with cardioprotective effect [35], and similar outcomes were observed in ZLN005+DOX group.

Alarmins are a set of ubiquitously present molecules mediating diverse physiological roles. Alarmins may play a dual role that can be protective or detrimental for cells in spatio-temporal context. Cell survival and proliferation is regulated by S100b, it has been shown to promote neuronal cells survival in picomolar to nanomolar quantities and cell death in micromolar concentrations [36]. Further, stimulation with S100b inhibits myogenic differentiation [37] and post DOX treatment; cardiomyocytes have a tendency to differentiate into fibroblast like phenotype with corresponding decrease in S100b levels. Intracellular S100b reportedly inhibited apoptosis in myoblast while playing a role in their differentiation [38]. In our present study, we observed similar trends where *S100b* transcript levels were decreased in DOX group and increased after ZLN005 (ZLN005+DOX group) treatment but the comparison was not statistically significant. HMGB1 is another alarmin investigated and is responsible for mediating cardiac injury [39, 40]. In contrast to our study i.e. DOX (10mg/kg, i.p.) with 1 week survival, Yao et al. administered DOX (20mg/kg, i.p.) with survival of 5 days [40] where they found increased HMGB1 protein expression in cardiac tissue along with increased circulating HMGB1 concentration in serum of DOX group compared to control group. Another study demonstrated differential binding pattern of HMGB1 to DNA with dose dependent response of DOX i.e. increased HMGB1-DNA binding at low DOX concentration and *vice versa* [41]. Cathepsin-B is a lysosomal protease that is associated with aggravation of symptoms in DOX injury model [42], Liu et al. reported increased cathepsin-B protein expression in cardiomyocyte cell line H9C2, post DOX (0.5uM, 24h) treatment [42]. Cathepsin-B is also known to mediate cardiac remodeling events [43] and play a role in progression of cardiomyopathy phenotype through cell death pathways [44]. However, in our study, we observed no significant variation in transcript expression levels of *HMGB1* and *cathepsin-B* in cardiac tissue and corresponding protein levels will be required to address these discrepancies.

During extracellular matrix remodeling components like fibronectin and laminin play an important role in deposition of collagen fibers within myocardium. This leads to extracellular matrix protein accumulation leading to stiffening of myocardium. Inhibition of fibronectin improves cardiac dysfunction and halts progression towards heart failure [45]. In our present study we found significant increased concentration of laminin and fibronectin proteins in heart tissue lysates in DOX group and it was restored to normal levels after ZLN005 treatment thereby circumventing the harmful DOX induced tissue remodeling process. Further, Col I/III ratio is an important factor involved in tissue remodeling associated with myocardial infarction and progression toward HF [46, 47]. In the present study, we found decreased Col I/III ratio in DOX group compared to control. The ZLN005 (ZLN005+DOX group) treatment improved the Col I/III ratio towards the control. All these data collectively demonstrated the potential tissue remodeling effect of PGC1 $\alpha$  that has not been reported previously.

The present study has not reported the data related to cardiac function. The echocardiography based cardiac function data (e.g. ejection fraction (EF), LVEDD (left ventricular end-diastolic dimension), LVESD (left ventricle end-systolic dimension), FS (fractional shortening) etc.) would be of great interest to understand the effect of PGC1 $\alpha$  agonist on the functional cardiac parameters and it is one of the limitations of the present study.

## Impact of research in the advancement of knowledge or benefit mankind

This study highlights the role of PGC1 $\alpha$  agonist (ZLN005) in mitigating cardiomyopathy phenotype by strengthening the redox balance, via mitigating DOX mediated oxidative stress, thereby preventing the harmful tissue remodeling effects and necroptosis. No study so far has reported cardioprotective action of this molecule in disease/ dysfunction model and the impact of PGC1 $\alpha$  in mediating cell death (particularly necroptosis) is novel finding of this study.

Cardiovascular diseases are accompanied by a cascade of events that involve extensive production of reactive oxygen species, cell death and tissue remodeling. This vicious cycle amplifies itself, leading to decline in cardiac performance, ultimately manifesting into disease onset. To provide cardioprotective impact it is vital to stop this series of events which is a strategy employed in our work.

From a Cardio-oncology point of view, currently dexrazoxane is the only drug approved by FDA that is used to confer cardioprotective impact when administered before DOX. However, it causes a dose dependent myelotoxicity that manifests into leukopenia, thrombocytopenia, neutropenia, granulocytopenia. Further, it is a category D drug that can lead to fetal toxicity, besides developing symptoms of superficial phlebitis, mucositis, kidney dysfunction, hair loss, localized pain at injection site, to mention few side effects. All these factors urge for an important need to look for alternatives.

In the current study ZLN005 showed improvement of cardiac structure by inhibition of necroptosis, oxidative stress and tissue remodeling. These observations are rare and valuable, since one drug is accounting for overall recovery. Use of multiple drugs simultaneously to inhibit specific mechanisms could lead to compromise of effective function, due to multiple drug-drug interactions in action. The targeted delivery of ZLN005 to heart can provide cardiovascular benefits, besides its role in mitigating DOX induced cardiotoxicity. The outcomes of such studies have potential for translation into clinics for the management of cardiac injury / disease condition for effective management of cardiovascular complications.

## Literature References

1. Primo, G.; Le Clerc, J. L.; Goldstein, J. P.; De Smet, J. M.; Joris, M. P., Cardiac transplantation for the treatment of endstage ischemic cardiomyopathy. *Advances in cardiology* **1988**, *36*, 293-7.
2. Report of the 1995 World Health Organization/International Society and Federation of Cardiology Task Force on the Definition and Classification of Cardiomyopathies. **1996**, *93* (5), 841-842.
3. Hudson, M. M.; Ness, K. K.; Gurney, J. G.; Mulrooney, D. A.; Chemaitilly, W.; Krull, K. R.; Green, D. M.; Armstrong, G. T.; Nottage, K. A.; Jones, K. E.; Sklar, C. A.; Srivastava, D. K.; Robison, L. L., Clinical ascertainment of health outcomes among adults treated for childhood cancer. *Jama* **2013**, *309* (22), 2371-2381.
4. Volkova, M.; Russell, R., 3rd, Anthracycline cardiotoxicity: prevalence, pathogenesis and treatment. *Current cardiology reviews* **2011**, *7* (4), 214-20.
5. Swain, S. M.; Whaley, F. S.; Ewer, M. S., Congestive heart failure in patients treated with doxorubicin: a retrospective analysis of three trials. *Cancer* **2003**, *97* (11), 2869-79.
6. Lefrak, E. A.; Pit'ha, J.; Rosenheim, S.; Gottlieb, J. A., A clinicopathologic analysis of adriamycin cardiotoxicity. **1973**, *32* (2), 302-314.
7. Shi, Y.; Moon, M.; Dawood, S.; McManus, B.; Liu, P. P., Mechanisms and management of doxorubicin cardiotoxicity. *Herz* **2011**, *36* (4), 296-305.
8. Zhang, S.; Liu, X.; Bawa-Khalfe, T.; Lu, L.-S.; Lyu, Y. L.; Liu, L. F.; Yeh, E. T. H., Identification of the molecular basis of doxorubicin-induced cardiotoxicity. *Nature Medicine* **2012**, *18* (11), 1639-1642.
9. Tang, D.; Kang, R.; Berghe, T. V.; Vandenabeele, P.; Kroemer, G., The molecular machinery of regulated cell death. *Cell Research* **2019**, *29* (5), 347-364.
10. Galluzzi, L.; Vitale, I.; Aaronson, S. A.; Abrams, J. M.; Adam, D.; Agostinis, P.; Alnemri, E. S.; Altucci, L.; Amelio, I.; Andrews, D. W.; Annicchiarico-Petruzzelli, M.; Antonov, A. V.; Arama, E.; Baehrecke, E. H.; Barlev, N. A.; Bazan, N. G.; Bernassola, F.; Bertrand, M. J. M.; Bianchi, K.; Blagosklonny, M. V.; Blomgren, K.; Borner, C.; Boya, P.; Brenner, C.; Campanella, M.; Candi, E.; Carmona-Gutierrez, D.; Cecconi, F.; Chan, F. K. M.; Chandel, N. S.; Cheng, E. H.; Chipuk, J. E.; Cidlowski, J. A.; Ciechanover, A.; Cohen, G. M.; Conrad, M.; Cubillos-Ruiz, J. R.; Czabotar, P. E.; D'Angiolella, V.; Dawson, T. M.; Dawson, V. L.; De Laurenzi, V.; De Maria, R.; Debatin, K.-M.; DeBerardinis, R. J.; Deshmukh, M.; Di Daniele, N.; Di Virgilio, F.; Dixit, V. M.; Dixon, S. J.; Duckett, C. S.; Dynlacht, B. D.; El-Deiry, W. S.; Elrod, J. W.; Fimia, G. M.; Fulda, S.; García-Sáez, A. J.; Garg, A. D.; Garrido, C.; Gavathiotis, E.; Golstein, P.; Gottlieb, E.; Green, D. R.; Greene, L. A.; Gronemeyer, H.; Gross, A.; Hajnoczky, G.; Hardwick, J. M.; Harris, I. S.; Hengartner, M. O.; Hetz, C.; Ichijo, H.; Jäättelä, M.; Joseph, B.; Jost, P. J.; Juin, P. P.; Kaiser, W. J.; Karin, M.; Kaufmann, T.; Kepp, O.; Kimchi, A.; Kitsis, R. N.; Klionsky, D. J.; Knight, R. A.; Kumar, S.; Lee, S. W.; Lemasters, J. J.; Levine, B.; Linkermann, A.; Lipton, S. A.; Lockshin, R. A.; López-Otín, C.; Lowe, S. W.; Luedde, T.; Lugli, E.; MacFarlane, M.; Madeo, F.; Malewicz, M.; Malorni, W.; Manic, G.; Marine, J.-C.; Martin, S. J.; Martinou, J.-C.; Medema, J. P.; Mehlen, P.; Meier, P.; Melino, S.; Miao, E. A.; Molkentin, J. D.; Moll, U. M.; Muñoz-Pinedo, C.; Nagata, S.; Nuñez, G.; Oberst, A.; Oren, M.; Overholtzer, M.; Pagano, M.; Panaretakis, T.; Pasparakis, M.; Penninger, J. M.; Pereira, D. M.; Pervaiz, S.; Peter, M. E.; Piacentini, M.; Pinton, P.; Prehn, J. H. M.; Puthalakath, H.; Rabinovich, G.

- A.; Rehm, M.; Rizzuto, R.; Rodrigues, C. M. P.; Rubinsztein, D. C.; Rudel, T.; Ryan, K. M.; Sayan, E.; Scorrano, L.; Shao, F.; Shi, Y.; Silke, J.; Simon, H.-U.; Sistigu, A.; Stockwell, B. R.; Strasser, A.; Szabadkai, G.; Tait, S. W. G.; Tang, D.; Tavernarakis, N.; Thorburn, A.; Tsujimoto, Y.; Turk, B.; Vanden Berghe, T.; Vandenabeele, P.; Vander Heiden, M. G.; Villunger, A.; Virgin, H. W.; Vousden, K. H.; Vucic, D.; Wagner, E. F.; Walczak, H.; Wallach, D.; Wang, Y.; Wells, J. A.; Wood, W.; Yuan, J.; Zakeri, Z.; Zhivotovsky, B.; Zitvogel, L.; Melino, G.; Kroemer, G., Molecular mechanisms of cell death: recommendations of the Nomenclature Committee on Cell Death 2018. *Cell Death & Differentiation* **2018**, *25* (3), 486-541.
11. Christidi, E.; Brunham, L. R., Regulated cell death pathways in doxorubicin-induced cardiotoxicity. *Cell Death & Disease* **2021**, *12* (4), 339.
12. Yu, X.; Ruan, Y.; Huang, X.; Dou, L.; Lan, M.; Cui, J.; Chen, B.; Gong, H.; Wang, Q.; Yan, M.; Sun, S.; Qiu, Q.; Zhang, X.; Man, Y.; Tang, W.; Li, J.; Shen, T., Dexrazoxane ameliorates doxorubicin-induced cardiotoxicity by inhibiting both apoptosis and necroptosis in cardiomyocytes. *Biochemical and biophysical research communications* **2020**, *523* (1), 140-146.
13. Erdogmus Ozgen, Z.; Erdinc, M.; Kelle, I.; Erdinc, L.; Nergiz, Y., Protective effects of necrostatin-1 on doxorubicin-induced cardiotoxicity in rat heart. *Hum Exp Toxicol* **2022**, *41*, 9603271211066066.
14. Kaczmarek, A.; Vandenabeele, P.; Krysko, D. V., Necroptosis: the release of damage-associated molecular patterns and its physiological relevance. *Immunity* **2013**, *38* (2), 209-23.
15. Chan, J. K.; Roth, J.; Oppenheim, J. J.; Tracey, K. J.; Vogl, T.; Feldmann, M.; Horwood, N.; Nanchahal, J., Alarmins: awaiting a clinical response. *The Journal of clinical investigation* **2012**, *122* (8), 2711-9.
16. Satish, S.; Philipose, H.; Rosales, M. A. B.; Saint-Geniez, M., Pharmaceutical Induction of PGC-1 $\alpha$  Promotes Retinal Pigment Epithelial Cell Metabolism and Protects against Oxidative Damage. *Oxidative medicine and cellular longevity* **2018**, *2018*, 9248640.
17. Dinulovic, I.; Furrer, R.; Di Fulvio, S.; Ferry, A.; Beer, M.; Handschin, C., PGC-1 $\alpha$  modulates necrosis, inflammatory response, and fibrotic tissue formation in injured skeletal muscle. *Skeletal Muscle* **2016**, *6* (1), 38.
18. Rius-Pérez, S.; Torres-Cuevas, I.; Millán, I.; Ortega Á, L.; Pérez, S., PGC-1 $\alpha$ , Inflammation, and Oxidative Stress: An Integrative View in Metabolism. *Oxidative medicine and cellular longevity* **2020**, *2020*, 1452696.
19. Liang, D.; Zhuo, Y.; Guo, Z.; He, L.; Wang, X.; He, Y.; Li, L.; Dai, H., SIRT1/PGC-1 pathway activation triggers autophagy/mitophagy and attenuates oxidative damage in intestinal epithelial cells. *Biochimie* **2020**, *170*, 10-20.
20. Peres Diaz, L. S.; Schuman, M. L.; Aisicovich, M.; Toblli, J. E.; Pirola, C. J.; Landa, M. S.; García, S. I., Short-term doxorubicin cardiotoxic effects: involvement of cardiac Thyrotropin Releasing Hormone system. *Life sciences* **2020**, *261*, 118346.
21. Sun, J.; Li, J. Y.; Zhang, L. Q.; Li, D. Y.; Wu, J. Y.; Gao, S. J.; Liu, D. Q.; Zhou, Y. Q.; Mei, W., Nrf2 Activation Attenuates Chronic Constriction Injury-Induced Neuropathic Pain via Induction of PGC-1 $\alpha$ -Mediated Mitochondrial Biogenesis in the Spinal Cord. *Oxidative medicine and cellular longevity* **2021**, *2021*, 9577874.
22. Xu, Y.; Kabba, J. A.; Ruan, W.; Wang, Y.; Zhao, S.; Song, X.; Li, J.; Pang, T., The PGC-1 $\alpha$  Activator ZLN005 Ameliorates Ischemia-Induced Neuronal Injury In Vitro and In Vivo. *Cellular and molecular neurobiology* **2018**, *38* (4), 929-939.
23. Wallace, K. B.; Sardão, V. A.; Oliveira, P. J., Mitochondrial Determinants of Doxorubicin-Induced Cardiomyopathy. *Circ Res* **2020**, *126* (7), 926-941.
24. Osataphan, N.; Phrommintikul, A.; Chattipakorn, S. C.; Chattipakorn, N., Effects of doxorubicin-induced cardiotoxicity on cardiac mitochondrial dynamics and mitochondrial function: Insights for future interventions. *Journal of cellular and molecular medicine* **2020**, *24* (12), 6534-6557.
25. Liu, Y.; Bai, H.; Guo, F.; Thai, P. N.; Luo, X.; Zhang, P.; Yang, C.; Feng, X.; Zhu, D.; Guo, J.; Liang, P.; Xu, Z.; Yang, H.; Lu, X., PGC-1 $\alpha$  activator ZLN005 promotes maturation of cardiomyocytes derived from human embryonic stem cells. *Aging* **2020**, *12* (8), 7411-7430.
26. Zhou, Q.; Xu, H.; Yan, L.; Ye, L.; Zhang, X.; Tan, B.; Yi, Q.; Tian, J.; Zhu, J., PGC-1 $\alpha$  promotes mitochondrial respiration and biogenesis during the differentiation of hiPSCs into cardiomyocytes. *Genes & diseases* **2021**, *8* (6), 891-906.
27. Brainard, R. E.; Facundo, H. T., Cardiac hypertrophy drives PGC-1 $\alpha$  suppression associated with enhanced O-glycosylation. *Biochimica et Biophysica Acta (BBA) - Molecular Basis of Disease* **2021**, *1867* (5), 166080.
28. Zhu, P.; Ma, H.; Cui, S.; Zhou, X.; Xu, W.; Yu, J.; Li, J., ZLN005 Alleviates In Vivo and In Vitro Renal Fibrosis via PGC-1 $\alpha$ -Mediated Mitochondrial Homeostasis. *Pharmaceuticals (Basel)* **2022**, *15* (4).
29. Shi, Z.; Wang, S.; Deng, J.; Gong, Z., PGC-1 $\alpha$  attenuates the oxidative stress-induced impaired osteogenesis and angiogenesis regulation effects of mesenchymal stem cells in the presence of diabetic serum. *Biochemistry and biophysics reports* **2021**, *27*, 101070.
30. Valle, I.; Alvarez-Barrientos, A.; Arza, E.; Lamas, S.; Monsalve, M., PGC-1 $\alpha$  regulates the mitochondrial antioxidant defense system in vascular endothelial cells. *Cardiovasc Res* **2005**, *66* (3), 562-73.
31. Di Minno, A.; Turnu, L.; Porro, B.; Squellerio, I.; Cavalca, V.; Tremoli, E.; Di Minno, M. N., 8-Hydroxy-2-Deoxyguanosine Levels and Cardiovascular Disease: A Systematic Review and Meta-Analysis of the Literature. *Antioxidants & redox signaling* **2016**, *24* (10), 548-55.
32. Thomas, M. C.; Woodward, M.; Li, Q.; Pickering, R.; Tikellis, C.; Poulter, N.; Cooper, M. E.; Marre, M.; Zoungas, S.; Chalmers, J., Relationship Between Plasma 8-OHdG and Cardiovascular Disease and Survival in Type 2 Diabetes Mellitus: Results From the ADVANCE Trial. **2018**, *7* (13), e008226.
33. Qin, F.; Lennon-Edwards, S.; Lancel, S.; Biolo, A.; Siwik, D. A.; Dorn, G. W.; Kang, Y. J.; Colucci, W. S., Cardiac-specific overexpression of catalase identifies hydrogen peroxide-dependent and -independent phases of myocardial remodeling and prevents the progression to overt heart failure in G $\alpha$ q-overexpressing transgenic mice. *Circulation. Heart failure* **2010**, *3* (2), 306-13.



34. Li, X.; Lin, Y.; Wang, S.; Zhou, S.; Ju, J.; Wang, X.; Chen, Y.; Xia, M., Extracellular Superoxide Dismutase Is Associated With Left Ventricular Geometry and Heart Failure in Patients With Cardiovascular Disease. **2020**, 9 (15), e016862.
35. van Deel, E. D.; Lu, Z.; Xu, X.; Zhu, G.; Hu, X.; Oury, T. D.; Bache, R. J.; Duncker, D. J.; Chen, Y., Extracellular superoxide dismutase protects the heart against oxidative stress and hypertrophy after myocardial infarction. *Free radical biology & medicine* **2008**, 44 (7), 1305-13.
36. Sorci, G.; Riuzzi, F.; Agneletti, A. L.; Marchetti, C.; Donato, R., S100B inhibits myogenic differentiation and myotube formation in a RAGE-independent manner. *Molecular and cellular biology* **2003**, 23 (14), 4870-81.
37. Tubaro, C.; Arcuri, C.; Giambanco, I.; Donato, R., S100B protein in myoblasts modulates myogenic differentiation via NF-kappaB-dependent inhibition of MyoD expression. *Journal of cellular physiology* **2010**, 223 (1), 270-82.
38. Tubaro, C.; Arcuri, C.; Giambanco, I.; Donato, R., S100B in myoblasts regulates the transition from activation to quiescence and from quiescence to activation and reduces apoptosis. *Biochimica et Biophysica Acta (BBA) - Molecular Cell Research* **2011**, 1813 (5), 1092-1104.
39. Andrassy, M.; Volz, H. C.; Igwe, J. C.; Funke, B.; Eichberger, S. N.; Kaya, Z.; Buss, S.; Autschbach, F.; Pleger, S. T.; Lukic, I. K.; Bea, F.; Hardt, S. E.; Humpert, P. M.; Bianchi, M. E.; Mairbäurl, H.; Nawroth, P. P.; Remppis, A.; Katus, H. A.; Bierhaus, A., High-Mobility Group Box-1 in Ischemia-Reperfusion Injury of the Heart. **2008**, 117 (25), 3216-3226.
40. Yao, Y.; Xu, X.; Zhang, G.; Zhang, Y.; Qian, W.; Rui, T., Role of HMGB1 in doxorubicin-induced myocardial apoptosis and its regulation pathway. *Basic research in cardiology* **2012**, 107 (3), 267.
41. Bosire, R.; Fadel, L.; Mocsár, G.; Nánási, P.; Sen, P.; Sharma, A. K.; Naseem, M. U.; Kovács, A.; Kugel, J.; Kroemer, G.; Vámosi, G.; Szabó, G., Doxorubicin impacts chromatin binding of HMGB1, Histone H1 and retinoic acid receptor. *Scientific reports* **2022**, 12 (1), 8087.
42. Liu, C.; Cai, Z.; Hu, T.; Yao, Q.; Zhang, L., Cathepsin B aggravated doxorubicin-induced myocardial injury via NF-κB signalling. *Molecular medicine reports* **2020**, 22 (6), 4848-4856.
43. Wu, Q. Q.; Xu, M.; Yuan, Y.; Li, F. F.; Yang, Z.; Liu, Y.; Zhou, M. Q.; Bian, Z. Y.; Deng, W.; Gao, L.; Li, H.; Tang, Q. Z., Cathepsin B deficiency attenuates cardiac remodeling in response to pressure overload via TNF-α/ASK1/JNK pathway. *American journal of physiology. Heart and circulatory physiology* **2015**, 308 (9), H1143-54.
44. Liu, C.; Yao, Q.; Hu, T.; Cai, Z.; Xie, Q.; Zhao, J.; Yuan, Y.; Ni, J.; Wu, Q. Q., Cathepsin B deteriorates diabetic cardiomyopathy induced by streptozotocin via promoting NLRP3-mediated pyroptosis. *Molecular therapy. Nucleic acids* **2022**, 30, 198-207.
45. Valiente-Alandi, I.; Potter, S. J.; Salvador, A. M.; Schafer, A. E.; Schips, T.; Carrillo-Salinas, F.; Gibson, A. M.; Nieman, M. L.; Perkins, C.; Sargent, M. A.; Huo, J.; Lorenz, J. N.; DeFalco, T.; Molkenin, J. D.; Alcaide, P.; Blaxall, B. C., Inhibiting Fibronectin Attenuates Fibrosis and Improves Cardiac Function in a Model of Heart Failure. *Circulation* **2018**, 138 (12), 1236-1252.
46. Querejeta, R.; López, B.; González, A.; Sánchez, E.; Larman, M.; Ubago, J. L. M.; Díez, J., Increased Collagen Type I Synthesis in Patients With Heart Failure of Hypertensive Origin. **2004**, 110 (10), 1263-1268.
47. Wei, S.; Chow, L. T. C.; Shum, I. O. L.; Qin, L.; Sanderson, J. E., Left and right ventricular collagen type I/III ratios and remodeling post-myocardial infarction. *Journal of Cardiac Failure* **1999**, 5 (2), 117-126.

Shipra

Signatures